TENSILE PROPERTIES OF A TITANIUM MODIFIED AUSTENITIC STAINLESS STEEL AND THE WELD JOINTS AFTER NEUTRON IRRADIATION --- K. Shiba, I. Ioka, S. Jitsukawa, S. Hamada, A. Hishinuma [Japan Atomic Energy Research Institute (JAERI)] and J. Pawel Robertson [Oak Ridge National Laboratory (ORNL)]

OBJECTIVE

To investigate the irradiation behavior on the tensile properties of a titanium-modified austenitic stainless steels (JPCA) and its weldments by the HFIR target and the spectrally tailored irradiation.

SUMMARY

Tensile specimens of a titanium modified austenitic stainless steel and its weldments fabricated with Tungsten Inert Gas (TIG) and Electron Beam (EB) welding techniques were irradiated to a peak dose of 19 dpa and a peak helium level of 250 appm in the temperature range between 200 and 400°C in spectrally tailored capsules in the Oak Ridge Research Reactor (ORR) and the High Flux Isotope Reactor (HFIR). The He/dpa ratio of about 13 appm/dpa is similar to the typical helium/dpa ratio of a fusion reactor environment. The tensile tests were carried out at the irradiation temperature in vacuum. The irradiation caused an increase in yield stress to levels between 670 and 800 MPa depending on the irradiation temperature. Total elongation was reduced to less than 10%, however the specimens failed in an ductile manner. The results were compared with those of the specimens irradiated using irradiation capsules producing larger amount of He. Although the He/dpa ratio affected the microstructural change, the impact on the post irradiation tensile behavior was rather small for not only base metal specimens but also for the weld joint and the weld metal specimens.

INTRODUCTION

Fe-Cr-Ni austenitic alloys are recognized to be the candidate alloys for the structural materials of the first walls of the blankets (FWB) for the fusion experimental reactors. The austenitic alloys will be used at temperatures below 400°C in the International Thermonuclear Experimental Reactor (ITER). The accumulated damage level to the end of life at the FWB position will be 1 to 30 displacements per atom (dpa) depending on the project. For instance, the maximum damage level is proposed to be 30 dpa for ITER Extended Performance Phase [1].

Microstructural evolution in the austenitic alloys is strongly affected by the helium due to nuclear transmutation reaction during neutron irradiation [2,3]. The ratio between the helium level and the displacement damage level (He/dpa) by fusion neutrons will be about 14 appmHe/dpa for Fe-Cr-Ni austenitic alloys. Fission neutron irradiation in the spectral tailoring capsules of the Oak Ridge Research Reactor (ORR) and the High Flux Isotope Reactor (HFIR) at Oak Ridge National Laboratory (ORNL) is capable to achieve the He/dpa ratio relevant to fusion neutrons by adjusting thermal and fast neutron flux ratio. The spectral tailored irradiation was planned to evaluate the effects of the He/dpa ratio and to estimate the irradiation induced property changes of austenitic alloys in a fusion reactor, and conducted in the Japan-US collaborative program for the fusion reactor materials development.

Since welding will be used for the fabrication of FWB, it is important to evaluate the irradiation response of the weldments. It has been reported that the helium embrittlement strongly depends on thesegregation of helium at grain boundaries [4]. Because welding often causes to the coarsening of grains, He embrittlement is one of the interesting subjects for the weldment of austenitic alloys after irradiation.

TABLE 1--Chemical compositions of alloys

	Fe	C	Si	Mn	P	S
JPCA	bal.	0.052	0.51	1.78	0.28	0.005
TIG wire	bal.	0.057	0.35	1.77	0.008	0.002

	Cr	Ni	Mo	Ti	N
JPCA	14.3	15.5	2.3	0.24	0.004
TIG wire	14.4	16.1	2.4	0.23	0.0095

TABLE 2--TIG welding condition

Voltage	Beam Current	Welding Speed	Wire Feed	Cover Gas
11 V	200 A (DC-SP)	8-10 cm/min	8-10 gram/min	Ar (20-25 l)

TABLE 3--EB welding condition

Accelerating Voltage	Beam Current	Welding Speed	Working Distance	Focal Length
60 kV	300 mA	500 mm/min	400 mm	370 mm

In this paper, the tensile properties of the base metal specimens irradiated in the spectrally tailored capsules compared with those irradiated at the target position producing large amount of helium, and the effect of He is evaluated. Also, tensile properties of the weld metal and the weld joint are examined to evaluate the irradiation performance of the weldments including the susceptibility to the He embrittlement.

EXPERIMENTAL PROCEDURES

Tungsten Inert Gas (TIG) and Electron Beam (EB) welded joints made of titanium modified austenitic stainless steel (JPCA) were investigated in this study. The chemical composition of JPCA is listed in TABLE 1. JPCA was used in the solution annealed (SA) condition (1120°C) for both welding and irradiation. The welding conditions of each type of welding are listed in TABLE 2 and TABLE 3. TIG welding was performed with the TIG wire of chemical composition listed in TABLE 1, and EB welded joints were fabricated without filler metal. No post-welding heat treatments (PWHT) were performed on either type of weldments.

Base metal (BM), weld metal (WM) and weld-joint (WJ) type specimens were prepared to investigate the irradiation behavior of welded joints. These types of specimens were machined from different locations of the welded joints as shown in FIG. 1. Weld metal type specimens were made of all weld metal and the tensile specimens were machined in parallel with the weld direction. Weld joint type specimens contain base metal, heat affected zones (HAZ) and weld metal in each specimen. Two types of sheet tensile specimens, SS-1 and SS-3 type, were employed in this experiment. The dimensions of each type of specimen are shown in FIG. 2 with the location of each part in a WJ type specimen; i.e. a fusion line is located at the center of an SS-3 and one half of the specimen is the weld metal in both TIG and EB weldments, while weld metal is located at the center of an SS-1 specimen and the fusion lines are an both sides of the weld metal. The length of the weld metal part of EB WJ specimens is about 3-5 mm, while that of TIG WJ specimens is about 5-10 mm in both types of specimens.

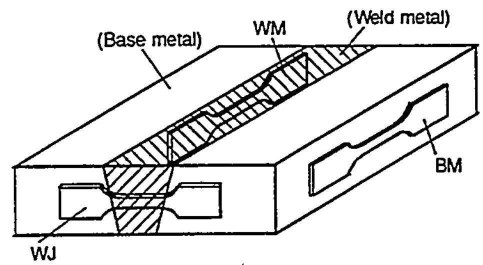

FIG. 1--The sampling location of specimens

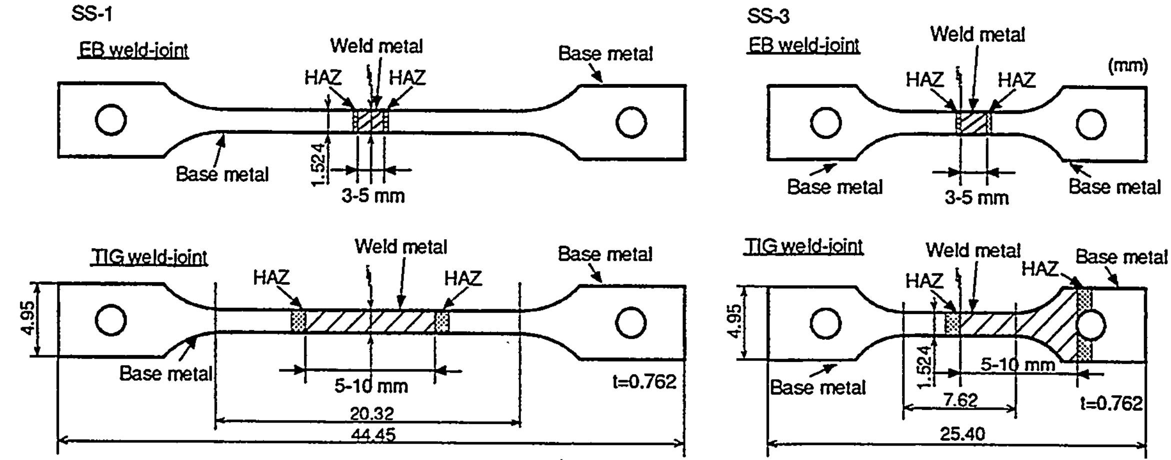

FIG. 2--The location of welded joint in WJ specimens

TABLE 4--Summary of Irradiation conditions (at capsule mid plane)

Capsules	Neutron Fluence (n/cm^2) Total	Thermal	Fast (E>0.1MeV)	Dose (dpa)	He (appm)	Irradiation Temperature (°C)
JP-10,11,13,16	7.9×10^{22}	3.1×10^{22}	2.1×10^{22}	17.5	1 080	300, 400, 500, 600
JP-14*	1.5×10^{23}	6.0×10^{22}	4.1×10^{22}	33.9	2 400	400, 500
JP-17	1.3×10^{22}	4.8×10^{21}	3.7×10^{21}	3.0	50	250
JP-20*	3.7×10^{22}	4.5×10^{22}	1.0×10^{22}	8.2	350	400
6J	2.4×10^{22}	6.7×10^{21}	6.8×10^{21}	6.9	90	60, 200
7J	2.7×10^{22}	8.1×10^{21}	9.5×10^{21}	7.4	120	330, 400
60J-1	4.0×10^{22}	4.7×10^{21}	1.9×10^{22}	11.6	130	60
330J-1	4.0×10^{22}	4.7×10^{21}	1.9×10^{22}	11.6	130	330
200J-1*	3.3×10^{22}	4.0×10^{21}	1.6×10^{22}	9.8	100	200
400J-1*	3.3×10^{22}	4.0×10^{21}	1.6×10^{22}	9.8	100	400
6J+60J-1	6.4×10^{22}	1.1×10^{22}	2.8×10^{22}	17.5	240	60
6J+200J-1*	5.7×10^{22}	8.7×10^{21}	2.3×10^{22}	16.7	190	200
7J+330J-1	6.7×10^{22}	1.3×10^{22}	2.9×10^{22}	19.0	250	330
7J+400J-1*	6.0×10^{22}	1.2×10^{22}	2.6×10^{22}	17.2	220	400

*Estimated from reactor power data.

Base metal, weld metal and weld joint specimens were irradiated at target and Removable Beryllium (RB) positions in the High Flux Isotope Reactor (HFIR). The spectral tailoring applied in this HFIR RB experiment is based on the 2-step nuclear reaction of ^{58}Ni, ^{58}Ni(n, γ)^{59}Ni(n, α)^{56}Fe in which the thermal neutron flux is controlled by using a thermal neutron shield. On the other hand, the HFIR target capsules are exposed to a much higher thermal flux generating much more helium in the specimens during the irradiation. The HFIR target capsules, HFIR-MFE-JP-10, 11, 13, 14, 16, 17 and 20 (JP10-20, hereafter)were irradiated up to 34 dpa at temperatures ranging from 250 to 600°C. Spectral tailoring was applied to the RB capsules, HFIR-MFE-200J-1, 330J-1 and 400J-1 at temperatures of 200, 330 and 400°C up to the dose of 12 dpa. The similar spectrally tailoring irradiation (ORR-MFE-6J, -7J) to about 7 dpa were carried out in ORR. Some of the ORR irradiated specimens were re-encapsuled in RB capsules. Therefore, the total dose level of the spectrally tailored irradiation was up to 19 dpa. Hereafter, the spectrally tailoring irradiation (ORR+RB irradiation) is called as "ORR/RB" in this paper. The detailed irradiation conditions of each capsule are summarized in TABLE 4 and further information of each irradiation capsule can be found in other reports [5-10]. The neutron fluence listed in TABLE 4 is the typical neutron fluence at the mid plane of each capsule. Some data in TABLE 4 were estimated from the reactor power data and the Greenwood's equations [11]. Since neutron flux has a distribution along the axial direction, the neutron fluence of each specimen varies according to its distance from the reactor mid plane. The damage and generated helium of each specimen were calculated using its position in the capsule. The dose level of each specimen is in the range of 2-34 dpa with 35-2380 appm He (He/dpa ~16-71) for JP10-20 and 7-19 dpa with 86-220 appm He (He/dpa ~11-16) for ORR/RB irradiation.

Tensile testing of irradiated specimens was carried out with an universal tensile machine in the hot laboratory at ORNL. The strain rates were 4×10^{-4} /s for SS-1 and 1×10^{-3} /s or 6×10^{-4} /s for SS-3 type specimens. Tensile testing was carried out at the nominal irradiation temperature of each irradiated specimen in vacuum. The 0.2% offset yield stress (YS), ultimate tensile stress (UTS), uniform elongation (Eu) and total elongation (Et) were obtained from the load-displacement curve of each specimen. The load drop just after yielding was neglected in the measurement of the uniform elongation. The fracture surface area of some specimens were measured with an optical microscope in order to calculate reduction of area (RA) and the fracture stress.

RESULTS AND DISCUSSION

Irradiation behavior of base metal

<u>The irradiation in the spectrally tailored capsules</u>

The SS-1 tensile specimens of JPCA SA were irradiated to 7 and 18 dpa in the temperature range between 200 to 400°C. The 0.2% offset yield stress levels of base metal (BM) specimens are plotted in FIG. 3.

It has been reported that the yield stress level saturates with the dose to a level depending on the temperature [1,12]. The yield stress levels exhibited almost no change between 7 and 18 dpa at 200°C. The yield stress level at 18 dpa seems to be close to the saturation level at 400°C. The yield strength increases rapidly with the first dose increment to 7 dpa, and both the total elongation and the uniform elongation decrease rapidly (see FIG.4 (e) and (g)) and the next dose increment between 7 and 18 dpa increased the yield stress only about 50% of that from 7 dpa. Evidence from related work indicates that the yield strength of 316 irradiated under similar conditions at 200-400°C has essentially saturated with dose by about 7 dpa [13].

The irradiation at 250°C with He/dpa ratios relevant to the fusion neutrons also conducted in the High Flux Reactor (HFR) at Petten and R2 reactor at Mol, and the results for JPCA SA are also plotted in FIG. 3 [14,15]. The yield stress level attained 655 MPa to 3 dpa, this was followed by an increase by only 150 MPa to 11 dpa. The tensile tests for the specimens irradiated at 330°C have been carried out for the specimens irradiated to one damage level of 7 dpa. Therefore, it is rather difficult to evaluate the saturation level. The yield stress levels of about 800 MPa at 330°C is, however, close to the saturation level at 250°C.

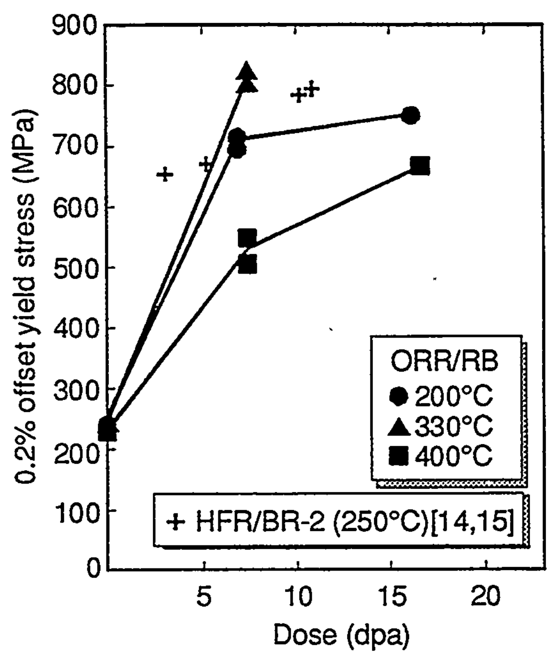

FIG. 3--Comparison of yield stress of PCA/JPCA irradiated in the different irradiation environments.[14,15]

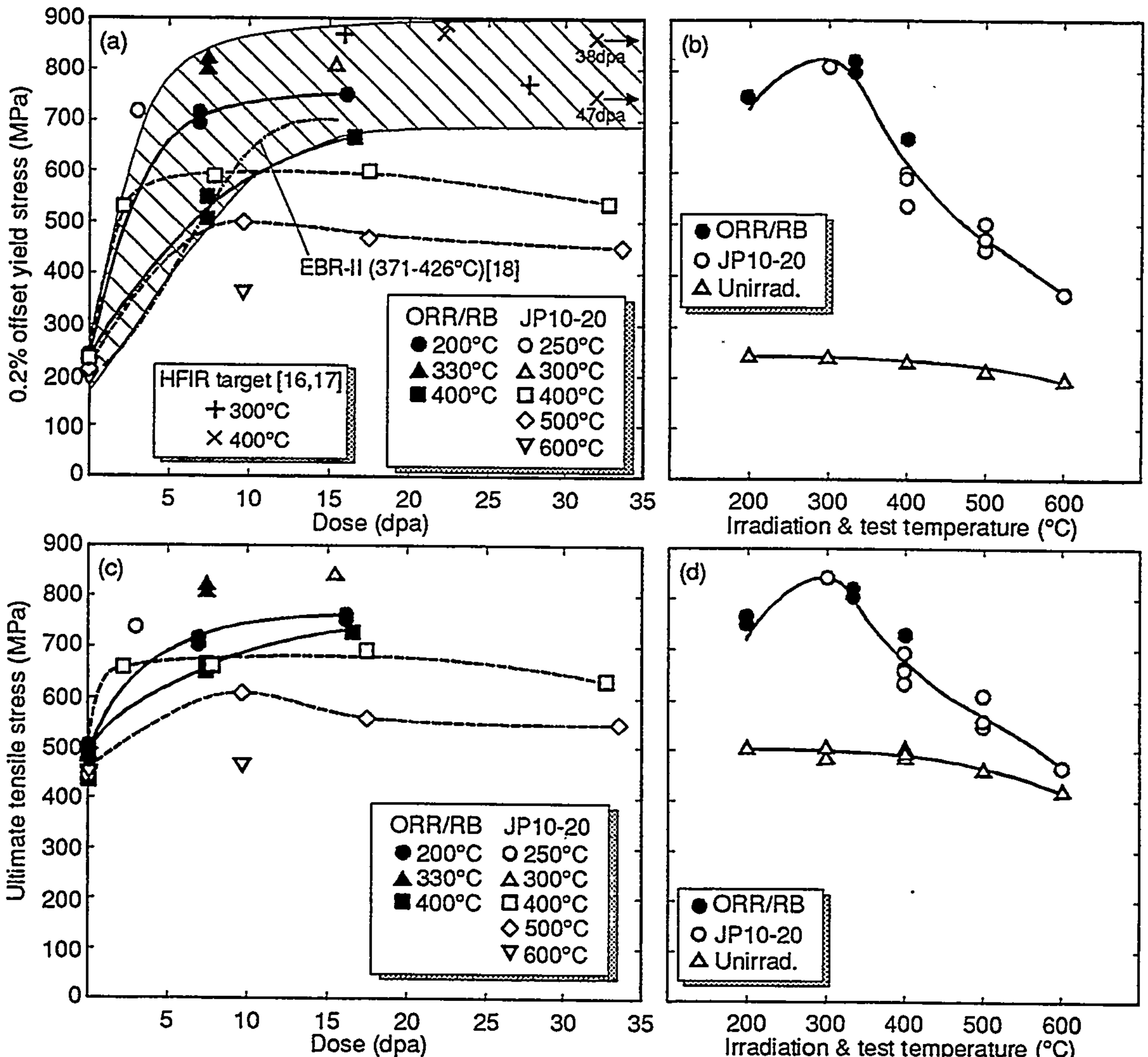

FIG. 4--Dose and temperature dependence of the tensile properties of JPCA irradiated in HFIR target capsules and spectrally tailored capsules. [16-18]

<u>The irradiation at the target position in the HFIR</u>

The SS-3 tensile specimens of JPCA SA were irradiated in JP10-20 to the dose levels ranging between 3 to 34 dpa at the temperatures ranging between 250 to 600°C. The He level is calculated to be 2400 appm for the specimens irradiated to 34 dpa. FIG. 4 (a) shows the yield stress levels of the JPCA SA before and after the irradiation (open symbols). The yield stress at 400°C increased by 300 MPa during the irradiation to only 2 dpa. This was followed by an increase by less than 100 MPa during the irradiation to 34 dpa. The saturation level at 400°C seems to be 550 MPa.

The tensile properties of JPCA SA irradiated at the HFIR target position have been reported previously [16,17]. The dose levels were ranged from 16 to 47 dpa. The yield stress of the previous experiments using round bar tensile specimen with the gauge section of 20.3 mm-long and 2.03 mm-diameter are also plotted in FIG. 4 (a). They are distributed in the hatched region, and indicating that the yield stress level saturated to dose levels between 10 and 20 dpa.

Plots for the spectral tailoring experiments (close symbols) also distributed in the hatched region, indicating that the helium effect on the yield stress level is rather small.

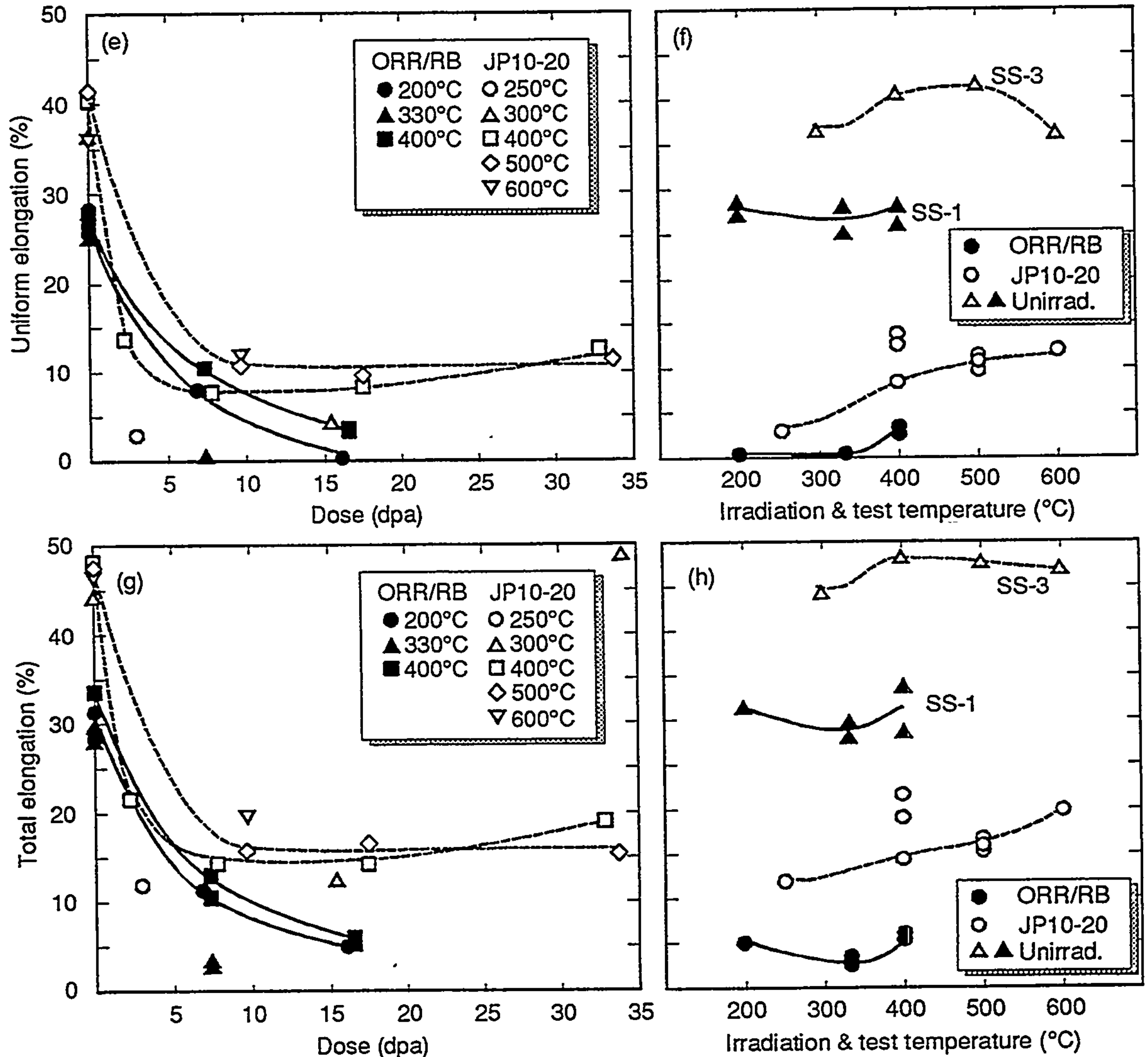

FIG. 4 (continued)--Dose and temperature dependence of the tensile properties of JPCA irradiated in HFIR target capsules and spectrally tailoring capsules.

The saturation level of the present results of HFIR target irradiation at 400°C is smaller than the previous results by more than 100 MPa. The temperature dependence at and above 400°C is rather large. The smaller saturation level may be resulted from that the irradiation temperature was higher than the expected temperature. Post-assembly inspection of capsules by X-ray radiograph technique, however, revealed that there was no disagreement between the measured and the designed gas gap dimensions.

Ultimate tensile strength, uniform elongation and total elongation are also plotted as functions of damage level and temperature in FIG. 4(c)-(h). The results with the damage levels higher than 7 dpa are plotted in the figures for the temperature dependence. Irradiation caused to increase UTS, as well as the yield stress. Total and uniform elongation decreased by irradiation. Higher yield stress accompanied with lower uniform elongation. The yield stress level decreased with temperature, while the uniform elongation increased.

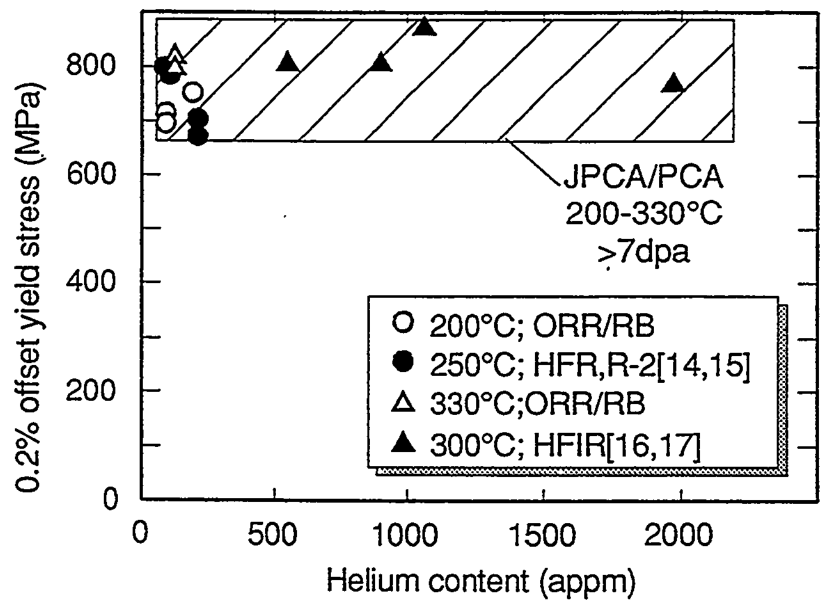

FIG. 5--Yield stress of PCA/JPCA irradiated in the different irradiation environments as a function of helium level.[14-17]

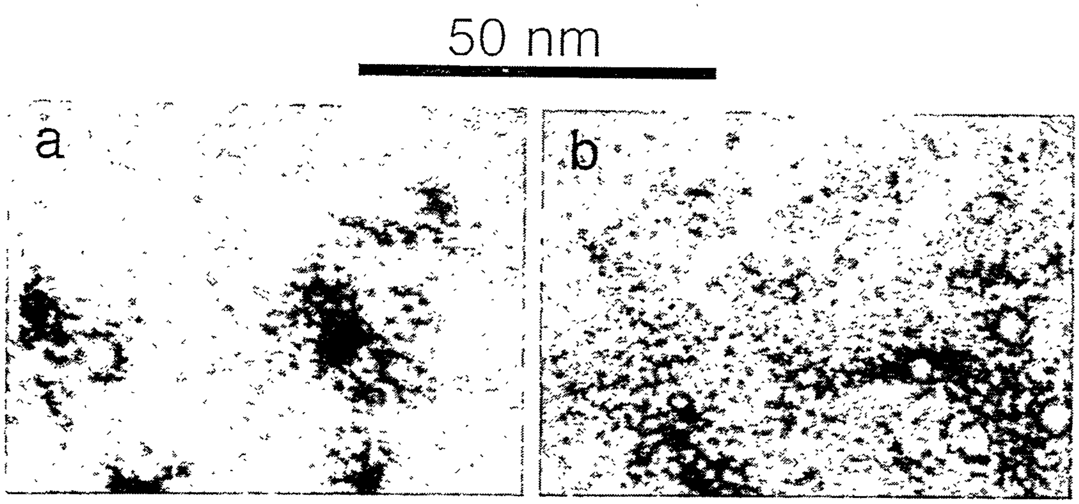

FIG. 6---Microstructure of JPCA irradiated at 400°C in (a) ORR 6J/7J (7 dpa) and (b) HFIR target capsules (17 dpa). [19,20]

TABLE 5--Cavities and dislocation loops in HFIR target and ORR irradiations

	Irradiation temperature	Cavities		Dislocation loops	
		Number density ($10^{23}/m^3$)	Average diameter (nm)	Number density ($10^{23}/m^3$)	Average diameter (nm)
HFIR 17 dpa (1100 appmHe)	400°C	6.9	2.5	0.4	36
ORR 7 dpa (130 appmHe)	400°C	0.3	2.6	2.2	27

Helium Effect on Tensile Properties

There is no significant difference between the levels of the yield stress after the irradiation in JP10-20 and those in ORR/RB. This is also true for UTS. On the other hand, the elongation for the specimens irradiated in ORR/RB are systematically smaller than those irradiated in JP10-20. The tensile specimen of SS-1 was irradiated in ORR/RB, while SS-3 was used for the JP10-20 irradiation. The sizes of SS-1 and SS-3 specimens are identical, except for the gauge length. Gauge length of SS-1 is 20.3 mm, which is 2.7 times longer than that of SS-3. The absolute value of elongation due to neck development is the same in both types of specimen, which correspond to 3% and 7.8% in total elongation for SS-1 and SS-3, respectively. The uniform elongation of these specimens also has some deference, as shown in FIG. 4 (f). One of the reason of this is the deformation occurred at the outside of the gauge section. Therefore, the elongation obtained from the different types of the specimens is not suitable to compare the ductility. As another index of ductility, reduction of area (RA) is applicable. The measurement of RA is in progress to compare the ductility of the specimens irradiated in each irradiation environments.

The yield stress data at or close to the saturation level are plotted against the helium levels in FIG. 5. No strong effect of helium on the yield stress level is seen.

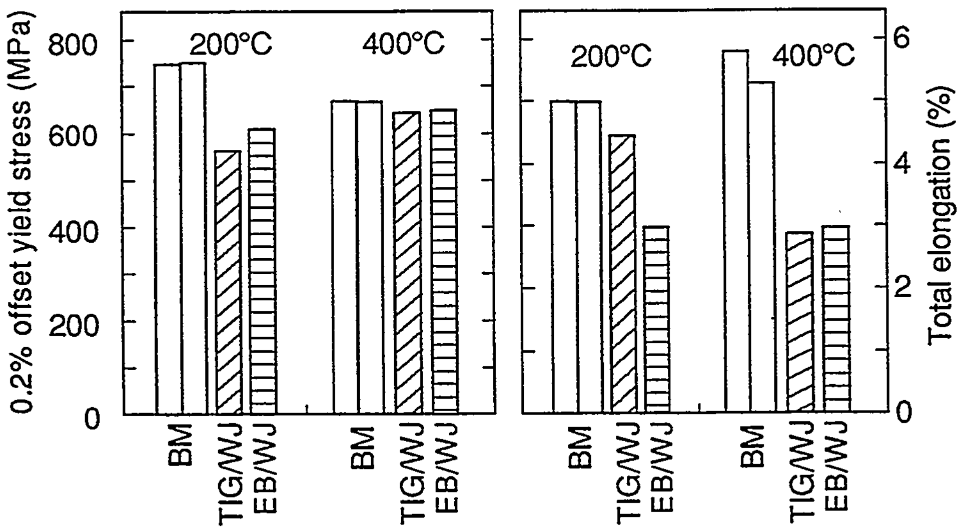

FIG. 7--The tensile properties of TIG and EB weld-joint specimens irradiated in spectrally tailoring capsules to 17 dpa.

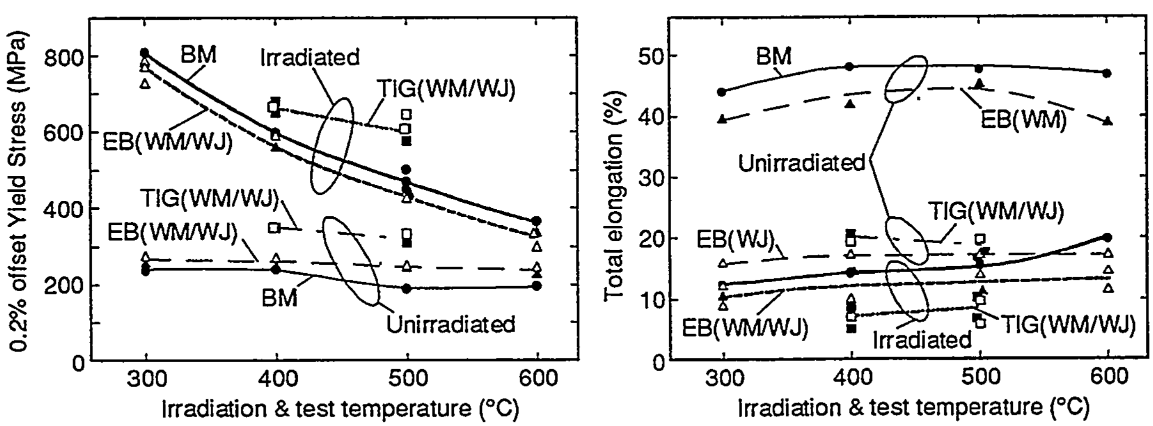

FIG. 8--Tensile properties of TIG and EB welded joints before and after irradiation to 8-34 dpa in HFIR target capsules.

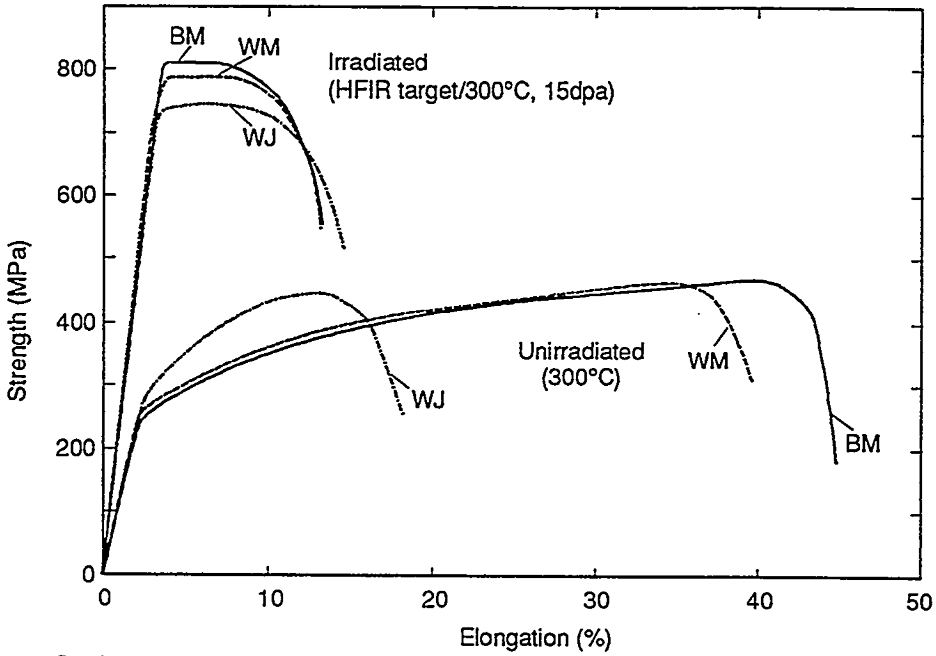

FIG. 9--Stress-Strain diagram of the JPCA SA and EB welded joints before and after irradiation in HFIR target capsules.

Microsructural observations on the specimens irradiated to 7 dpa in ORR/RB and those irradiated to 17 dpa in JP10-20 have been carried out. The tensile specimens irradiated in ORR/RB to 7 dpa and in JP10-20 to 17 dpa exhibited similar levels ranged from 500 to 550 MPa at 400°C. FIG. 6 shows TEM images in the kinematical condition [19,20]. The number densities and the diameters of the dislocation loops and the cavities observed in the specimens irradiated at 400°C in JP10-20 and ORR/RB are summarized in Table 5. The number density of cavities after the irradiation in JP10-20 is about twenty times higher than that of in ORR irradiation. In addition, more dislocation loops developed in the spectrally tailored irradiation. These differences in the microstructure suggest the hardening observed in both HIFR target and ORR/RB irradiation might be caused by the different mechanism; i. e. the irradiation hardening was strongly affected by cavities in JP10-20 irradiation, while it was caused by the frank loops mainly in ORR/RB irradiation, in spite of their similar yield stress levels.

The performance of the weld metal and the weld joint

FIG. 7 shows the yield stress and the total elongation of weld joint specimens of JPCA SA irradiated to 18 dpa in ORR/RB at 200 and 400°C. The results of JPCA SA base metal specimens are also plotted with those of the weld joint specimens of TIG and EB in the figure. The TIG WJ and EB WJ specimens exhibited slightly lower yield stress levels than that of base metal. This is similar to the result for the WJ specimens of 316 stainless steel irradiated to 7 dpa in MFE6/7J [21].

The total elongation of the JPCA TIG WJ and the EB WJ specimens are about 3%. This values are also close to those of the 316 TIG WJ and EB WJ.

The tensile properties of weldments irradiated in JP10-20 at temperatures ranging between 300 and 600°C to a damage level of about 17 dpa are plotted in FIG. 8. The yield stress levels and the total elongation of the weldments of JPCA with TIG and EB welding techniques are plotted with JPCA SA base metal. Results for the unirradiated specimens are also plotted in the figure. The yield stress levels of the TIG WM and WJ specimens were higher than base metal before and after the irradiation. The position of fracture

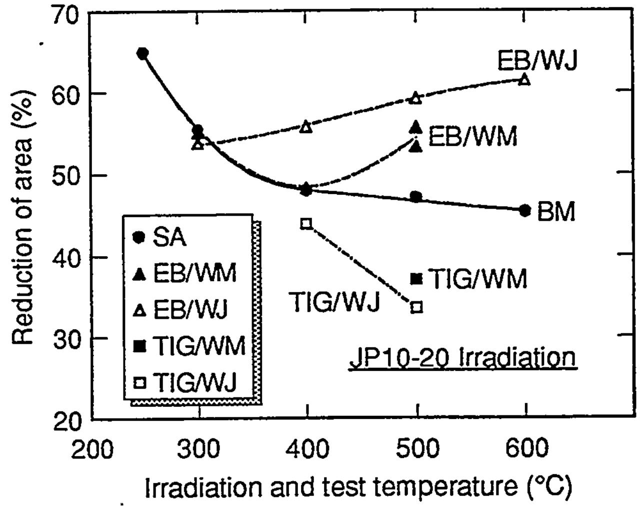

FIG. 10--Reduction of area of TIG and EB welded joints of JPCA SA irradiated to 3-18 dpa in HFIR target capsules.

has not been examined yet, however the lower yield stress levels for the EB welded specimens indicates that plastic deformation had mainly occurred in the weld metal region.

As indicated in FIG. 9, the elongation values of the WJ specimens before irradiation were often significantly smaller than those of the base metal specimens. The smaller elongation value for the WJ may be caused by the localized deformation in the weld metal region comparing with those of the heat affected zone and the base metal region. The deformation behaviors of the weld metal, the heat affected zone and the base metal regions in the WJ specimens are different. Therefore, the significance of the elongation values of the WJ specimens are not quite clear. On the other hand, the value of the reduction of area (RA) indicates the ductility level where fracture occurred.

The reduction of area can also be used as an indication of the ductility of the welded specimens. The RA values after the irradiation in JP10-20 are shown in FIG. 10. Note that while the irradiated RA values of the EB WM and WJ specimens are equal to or higher than the RA values of the base metal, the total elongation (FIG. 8) of the EB WM and WJ specimens were slightly less than the base metal. All the RA values are rather large suggesting the residual ductility level after irradiation is high enough for the application to fusion reactor components.

The welding often causes to form coarse grains at the heat affected zone and in the weld metal region. Because the He embrittlement is accompanied with the grain boundary separation, the welding may increase susceptibility to He embrittlement. The RA for EB/WJ specimens irradiated to 17 dpa with a helium levels of 1080 appm are revealed to be large and are higher than those of JPCA SA even at the highest temperature of 600°C.

CONCLUSION

The tensile properties of the base metal and TIG and EB welded joints of JPCA irradiated in HFIR target capsules and spectrally tailored capsules were studied.

1. The post irradiation strengths and the elongation values tend to saturate with the displacement damage at the temperatures below 400°C. No large effect of helium on the saturation levels is obtained.
2. The tensile properties of welded joints were very similar to those of the base metal. The weld metal and the weld joint specimens exhibited the same temperature and dose dependence as the base metal after irradiation.
3. Reduction of area observed in welded joints suggests weldments still retain enough ductility after irradiation.

ACKNOWLEDGMENTS

The authors appreciate the ORNL hot laboratory staff for the testing of irradiated specimens. We also thank to technicians of M&C division for their great assistance to the completion of this research.

This research was sponsored by the Japan Atomic Energy Research Institute and the Office of Fusion Energy Sciences, U.S. Department of Energy, under contract DE-AC05-96OR22464 with Lockheed Martin Energy Research Corporation.

REFERENCES

[1] Tavassoli, A.A., "Assessment of austenitic stainless steels", Fusion Engineering and Design 29 (1995), 371-390.

[2] Stoller, R.E. and Odette, G.R., "The effect of helium on swelling in stainless steel: influence of cavity density annd morphology", Effects of Radiation on Materials: 11th International Symposium, ASTM STP 782, F.R. Brager, and J.S. Perrin, Eds., American Society For Testing and Materials, Philadelphia, (1982) 275-294.

[3] Rowcliffe, A.F., Hishinuma, A., Grossbeck, M.L. and Jitsukawa, S, "Radiation effects at fusion reactor He:dpa ratios", J. Nucl. Mater. 179-181 (1991) 125-129.

[4] Kesternich, W. and Nandedkar, R.V., "On the role of helium in high temperature embrittlement of irradiated austenitic steels", Effects of Radiation on Materials: 14th International Symposium, ASTM STP 1046, N.H. Packan, R.E. Stoller and A.S. Kumar, Eds., American Society For Testing and Materials, Philadelphia, (1990) 284-294.

[5] Greenwood, L.R. and Ratner, R.T., "Neutron dosimetry and calculation for the JP-10, 11, 13 and 16 experiments in HFIR" Fusion Reactor Material Semiannual Progress Report, DOE/ER-0313/19, Office of Fusion Energy (1995) 281-283.

[6] Greenwood, L.R. and Baldwin, C.A., "Neutron dosimetry and calculation for the JP-17, 18 and 19 experiments in HFIR", Fusion Reactor Material Semiannual Progress Report, DOE/ER-0313/19, Office of Fusion Energy (1995) 286-290.

[7] Greenwood, L.R. Baldwin, C.A. and Oliver, B.M., "Neutron dosimetry, damage calculations and helium measurements for the HFIR-MFE-60J-1 and MFE-330J-1 spectral tailoring experiments", Fusion Reactor Material Semiannual Progress Report, DOE/ER-0313/17, Office of Fusion Energy (1994) 28-34.

[8] Pawel, J.E., Lenox, K.E. and Ioka, I., "Status of DOE/JAERI collaborative program Phase II and Phase III capsules" Fusion Reactor Material Semiannual Progress Report, DOE/ER-0313/19, Office of Fusion Energy (1995) 312-313.

[9] Greenwood, L.R., "Neutron Dosimetry and Damage Calculations for the ORR-MFE 7J Experiment" Fusion Reactor Material Semiannual Progress Report, DOE/ER-0313/6, Office of Fusion Energy (1989) 23-25.

[10] Greenwood, L.R., "Neutron Dosimetry and Damage Calculations for the ORR-MFE 6J Experiment" Fusion Reactor Material Semiannual Progress Report, DOE/ER-0313/8, Office of Fusion Energy (1990) 34-42.

[11] Greenwood, L.R., "A new calculation of thermal neutron damage and helium production in nickel", J. Nucl. Mater. 115 (1983) 137-142.

[12] Horsten, M.G. and de Vries, M.I, "Irradiation hardening and loss of ductility of type 316L(N) stainless steel plate material due to neutron-irradiation", Effects of Radiation on Materials: 17th International Symposium, ASTM STP 1270, D.S. Gelles, R.K. Nanstad, A.S. Kumar, and E.A. Little, Eds., American Society for Testing and Materials, 1995. (in press)

[13] Pawel, J.E., Ioka, I., Rowcliffe, A.F., Grossbeck, M.L. and Jitsukawa, S., "Temperature Dependence of the Deformation Behavior of 316 Stainless Steel after Low Temperature Neutron

Irradiation", Effects of Radiation on Materials: 18th International Symposium, ASTM STP 1325, R.K. Nanstad, M.L. Hamilton, F.A. Garner and A.S. Kumar, Eds., American Society for Testing and Materials, 1997. (these proceedings)

[14] Elen, J.D. and Fenici, P., "Fast neutron irradiation hardening of austenitic stainless at 250°C", J. Nucl. Mater. 191-194 (1992) 766-770.

[15] Jitsukawa, S., Grossbeck, M.L. and Hishinuma, A., "Stress-strain relations of irradiated stainless steels below 673K", J. Nucl. Mater. 191-194 (1992) 790-794.

[16] Tanaka, M.P., Hishinuma, A., Hamada, S. and Grossbeck, M.L., "Post irradiation tensile and fatigue behavior of austenitic PCA stainless steels irradiated in HFIR", J. Nucl. Mater. 155-157 (1988) 957-962.

[17] Hishinuma, A. and Jitsukawa, S., "Radiation damage of HFIR-irradiated candidate stainless steels for fusion applications", J. Nucl. Mater. 169 (1989) 241-248.

[18] Brager, H.R., Blackburn, l.D. and Garner, F.A., "The dependence on disolacement rate of radiation-induced changes in microstructure and tensile properties of ANSI 304 and 316",J. Nucl. Mater. 122-123 (1984) 332-337.

[19] Sawai, T., Shiba, K. and Hishinuma, A., "Microstructural Observation on HFIR-irradiated Austenitic Stainless Steels Including Welds from JP9-16" Fusion Reactor Material Semiannual Progress Report, DOE/ER-0313/19, Office of Fusion Energy (1995) 217-222.

[20] Sawai, T., Maziasz, P.J., Kanazawa, H. and Hishinuma, A., "Microstructural evolution of austenitic stainless steels irradiated in spectrally tailored experiment in ORR at 400°C", J. Nucl. Mater. 191-194 (1992) 712-716.

[21] Jitsukawa, S., Maziasz, P.J., Ishiyama, T., Gibson, L.T. and Hishinuma, A., "Tenisile properties of austenitic stainless Steels and their weld joints after irradiation by the ORR-spectrally-tailoring experiment", J. Nucl. Mater. 191-194 (1992) 771-775.